

Unraveling Water Structure Inside and Between Nanocapsules

Marc Henry¹

Received May 2, 2003

Among Achim Müller's prolific crystal structure database, we have selected two crystalline phases in order to perform a whole and complete characterization of water structure at the nanometer scale. The first chosen example involves the $\text{Na}_3(\text{NH}_4)_{12}[\text{Mo}_{57}\text{Fe}_6(\text{NO})_6\text{O}_{174}(\text{OH})_3(\text{H}_2\text{O})_{24}] \cdot 76\text{H}_2\text{O}$ compound synthesized and characterized in 1994. Some very interesting yet unnoticed water clusters may be evidenced in the voids generated by the stacking of the polyanionic units. Among them, we have been able to characterize a pure water crown $(\text{H}_2\text{O})_{18}$, a loose association of three strongly solvated ammonium ions $[\text{H}_3\text{N}-\text{H} \cdots \text{OH}_2]^+$ mediated by two water dimers and one water molecule, a perfectly planar alternating six-member ring $[(\text{NH}_4)_3(\text{H}_2\text{O})_3]^{3+}$, a puckered chair-shaped hexagonal ring $[(\text{NH}_4)_2(\text{H}_2\text{O})_4]^{3+}$ and two triangular pyramidal water tetramers $(\text{H}_2\text{O})_4$. It was also shown that the crown and the chair ring was involved through further hydrogen bonding into the formation of a quite novel supra-molecular layer modeling the structure of water in contact with a polyelectrolyte. The second example involves the $(\text{gua})_{32}[\text{Mo}_{132}\text{O}_{372}(\text{H}_2\text{O})_{72}(\text{SO}_4)_{10}(\text{H}_2\text{PO}_2)_{20}(\text{gua})_{20}] \cdot n\text{H}_2\text{O}$ compound synthesized and characterized in 2002. Here, we provide for the first time a complete structural analysis of all the various hydrogen bond patterns encountered in this system. Among them we may cite, an intramolecular web covering the internal cavity, an intramolecular finite system involving the guanidinium cations and the nine-member ring pores of the Mo_{132} shell and a central pure water cluster of one hundred water molecules. In this last case, the evolution of the hydrogen bond strengths on a per H-bond basis or within supramolecular aggregates $[(\text{H}_2\text{O})_{20}$, $[(\text{H}_2\text{O})_{40}$, and $[(\text{H}_2\text{O})_{100}]$ is quantitatively studied from standpoints involving both geometry (H-O...O bond angles distribution) and energy (partition functions). A survey of other crystalline phases involving water clusters is also presented. It is hoped that the study of these new clusters in a very next future will allow us to solve the well-known water puzzling behaviors.

¹ Solid State Molecular Tectonics, UMR CNRS/ULP 7140, Institut Le Bel, Université Louis Pasteur, 4, Rue Blaise Pascal, 67070 Strasbourg Cedex, France.

INTRODUCTION

For many years, Prof. Achim Müller has provided the scientific community with the most exciting and fascinating nano-objects. Since the early discovery in 1826 by Berzelius of the ammonium 12-molybdophosphate $(\text{NH}_4)_3[\text{PMo}_{12}\text{O}_{40}] \cdot n\text{H}_2\text{O}$ [1] up to the publication of M. T. Pope's book [2] in 1983, the largest polyanionic species ever synthesized contained at most forty transition metal atoms (Fig. 1). About ten years later, in 1992, the largest isolated species was a polyoxoalkoxomolybdate containing only forty two molybdenum atoms [3]. Thanks to Achim's work the following ten years up to now were particularly rewarding. The water clusters tale started with the synthesis and isolation in 1994 of $(\text{NH}_4)_{21}[\text{Mo}_{57}\text{V}_6(\text{NO})_6\text{O}_{180}(\text{OH})_3(\text{H}_2\text{O})_{18}] \cdot 65\text{H}_2\text{O}$ [4] and of $\text{Na}_3(\text{NH}_4)_{12}[\text{Mo}_{57}\text{Fe}_6(\text{NO})_6\text{O}_{174}(\text{OH})_3(\text{H}_2\text{O})_{24}] \cdot 76\text{H}_2\text{O}$ [5]. At that time, it was already noticed that these highly symmetrical heavily hydrated giant clusters displayed unusual cavities, raising the question of the possible existence of a host-guest chemistry based on water molecules. One year later a real breakthrough in nuclearity occurred with the synthesis and structural characterization of the first giant wheel $(\text{NH}_4)_{14}[\text{Mo}_{154}(\text{NO})_{14}\text{O}_{420}(\text{OH})_{28}(\text{H}_2\text{O})_{70}] \cdot 65\text{H}_2\text{O}$ characterized by an outer diameter of 3.4 nm and a thickness of 1.5 nm [6]. Two years later removal of the NO ligands allows to get a still larger ring (4.1 nm in diameter and 1.3 nm in thickness) containing 176 Mo-atoms: $[(\text{MoO}_3)_{176}(\text{H}_2\text{O})_{80}\text{H}_{32}] \cdot 400\text{H}_2\text{O}$ [7, 8] and $\text{Na}_{32}[(\text{MoO}_3)_{176}(\text{H}_2\text{O})_{63}(\text{CH}_3\text{OH})_{32}] \cdot 600\text{H}_2\text{O}$ [9]. On one hand, these structures are fascinating owing to their pretty large internal cavity size (ca. 2.0 nm for Mo_{154} and ca. 2.3 nm for Mo_{176}). On the other hand, they are quite deceptive, as these cavities are found to be virtually empty through X-ray diffraction. In fact, shells of highly organized water molecules are easily detected very close to the wheel (producing a negative image of the ring). It would then be very surprising that these water molecules would remain free of any hydrogen bonding with other partners located near the center of the wheel. It is thus highly probable that a huge amount of protic solute species is indeed trapped inside these cavities and that a high degree of disorder is probably responsible for their silent behavior in X-ray diffraction. Another problem with these compounds lies in the incredibly large number of atoms in the unit cells, making them truly inorganic analogs of proteins. Accordingly, even for our very highly efficient PACHA algorithm [10–12] running on a 2-GHz clocked pentium-4 processor, optimization of all the H-atoms coordinates for these wheels would take several months of CPU-time. Consequently, time is not yet ripe for studying the self-organization of such nano-objects and one has to wait for a parallel version of our PACHA algorithm and for further development of NMR techniques for solving crystalline structures [13].

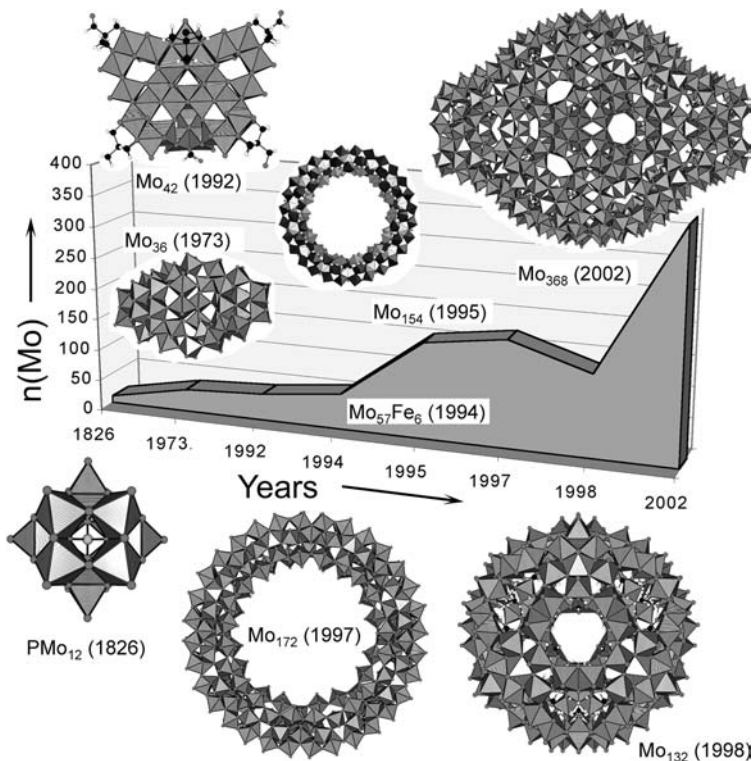


Fig. 1. The molybdenum-based polyanionic story. Achim Müller's group in Bielefeld synthesized most interesting phases in the past ten years.

Fortunately, at quite the same time, A. Müller's group was able to synthesize and solve the structure of an inorganic super fullerene and keplerate $(\text{NH}_4)_{21}[\text{Mo}_{132}\text{O}_{372}(\text{CH}_3\text{COO})_{30}(\text{H}_2\text{O})_{72}] \cdot 300\text{H}_2\text{O}$ [14]. For the first time, a sufficient amount of water molecules (but still highly disordered) was characterized at the center of the cavity allowing to unravel an amazing amorphous low-density ($\rho = 0.356 \text{ g} \cdot \text{cm}^{-3}$) water cluster formed of 59 H_2O molecules. Thanks to the PACHA algorithm, it was recently possible to take quantitatively into account this disorder, allowing a full characterization of the complex underlying H-bond pattern [15] characterized by a quite strong mean H-bond energy $\langle E_{\text{HB}} \rangle \sim -32 \text{ kJ} \cdot \text{mol}^{-1}$ [11]. Very soon after this discovery, it was found that the acetate linker was not mandatory in this kind of structure and may be easily substituted by formate ions [16], sulfate or hypophosphite ions [17]. In particular, the use of sulfate ions have permitted the isolation and characterization of the super-giant "blue lemon of Bielefeld," a nano-hedgehog containing

368 Mo-Atoms: $\text{Na}_{48}[\text{Mo}_{368}\text{O}_{1032}(\text{SO}_4)_{48}(\text{H}_2\text{O})_{24}] 1000\text{H}_2\text{O}$ [18]. It was also shown that part of molybdenum atoms may be substituted by iron atoms [19] or even removed leading to a smaller cage $[\text{Mo}_{102}\text{O}_{282}(\text{CH}_3\text{COO})_{12}(\text{H}_2\text{O})_{78}] 150\text{H}_2\text{O}$ [20]. Finally and quite recently, the replacement of ammonium counter-ions by sodium and/or guanidinium cations has shown that it was possible to play with the structure of the encapsulated cluster [21], allowing in one remarkable case to remove completely the disorder of the central water cluster [22].

It is not the aim of this contribution to review all the numerous other crystalline phases synthesized by A. Müller's group. We have here selected only those phases that are related by the occurrence of encapsulated water clusters of variable geometry. Even, in this restricted family of polyanions there is room for a considerable amount of work on each case. To further demonstrate this point we have limited ourselves to only two crystalline phases. The first one, $\text{Na}_3(\text{NH}_4)_{12}[\text{Mo}_{57}\text{Fe}_6(\text{NO})_6\text{O}_{174}(\text{OH})_3(\text{H}_2\text{O})_{24}] 76\text{H}_2\text{O}$ is already a quite old lady [5], but as will be shown below, she hides under her breast some amazing yet unrecognized water structures. It is a great pleasure for me to unravel for the first time the structure of these new clusters in this special issue published in honor of his 65th birthday. This first example will demonstrate the importance of Achim's work for future research with a mostly unexplored scientific database, from which the fascinating water structure puzzle will at last be solved. The second example is on the contrary devoted to one of the latest Achim's babies, an unprecedented well-organized water cluster containing exactly 100 molecules. In this case, we will make a full structural study of this nano-object under two major structural constraints: encapsulated versus free state.

$\text{Na}_3(\text{NH}_4)_{12}[\text{Mo}_{57}\text{Fe}_6(\text{NO})_6\text{O}_{174}(\text{OH})_3(\text{H}_2\text{O})_{24}] 76\text{H}_2\text{O}$: A JEWEL CASE

At the very beginning of the story was the crystalline phase $\text{Na}_3(\text{NH}_4)_{12}[\text{Mo}_{57}\text{Fe}_6(\text{NO})_6\text{O}_{174}(\text{OH})_3(\text{H}_2\text{O})_{24}] \cdot 76\text{H}_2\text{O}$ obtained after mixing of $\text{Na}_2\text{MoO}_4 \cdot 2\text{H}_2\text{O}$ and $\text{Fe}(\text{NO}_3)_3 \cdot 9\text{H}_2\text{O}$ in the presence of hydroxylamine $\text{NH}_2\text{OH} \cdot \text{HCl}$ [5]. As shown in the top of Fig. 2, the main point of interest in 1993 was the cluster anion made from three $[\text{Mo}(\mu\text{-H}_2\text{O})_2(\mu\text{-OH})\text{Mo}]^{9+}$ moieties condensed with three Mo_{17} units (based on two $[\text{Mo}(\text{NO})(\text{H}_2\text{O})]^{3+}$ pentagonal bipyramids fused with 15 MoO_6 octahedra) and six $[\text{Fe}^{\text{III}}\text{O}_4(\text{OH}_2)_2]$ octahedra. A good way of characterizing such a nano-object is to compute the following quantities: radius of the smallest sphere including all the matter R_{ext} , average density $\rho = 3M/(4\pi R_{\text{ext}}^3)$ moment of inertia (I_A , I_B , and I_C) along the three principal axes, molecular volume v_{mol} and surface s_{mol} . All these metrical data may be easily deduced from the knowledge of the molar mass M and molecular

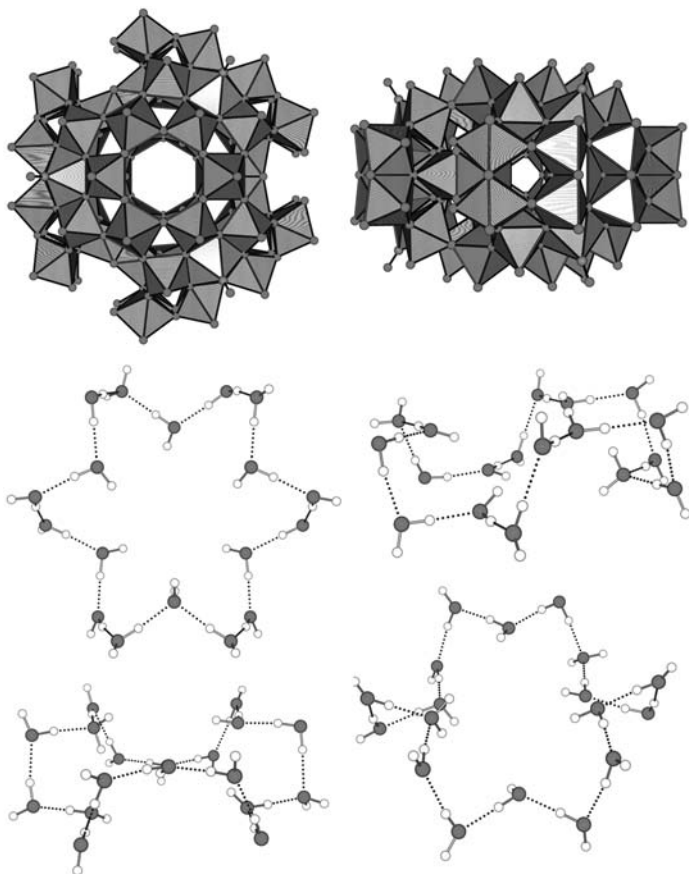


Fig. 2. The $[\text{Mo}_{57}\text{Fe}_6(\text{NO})_6\text{O}_{174}(\text{OH})_3(\text{H}_2\text{O})_{24}]$ cluster and its associated $(\text{H}_2\text{O})_{18}$ water crown lying surrounding the polyanion.

structure and from a set of van der Waals radii using Monte-Carlo algorithms for volumes [23] or surfaces [24]. In the present case, we have selected the following standard van der Waals radii: $\text{H} = 120 \text{ pm}$, $\text{N} = 155 \text{ pm}$, $\text{O} = 152 \text{ pm}$, and $\text{Fe} = \text{Mo} = 200 \text{ pm}$. This set of radii leads to: $R_{\text{ext}} = 12.27 \text{ \AA}$ (bulk volume 7734.6 \AA^3), $\rho = 1.975 \text{ g} \cdot \text{cm}^{-3}$, $I_A = 78.2 \times 10^{-41} \text{ kg} \cdot \text{m}^2$, $I_B = I_C = 53.4 \times 10^{-41} \text{ kg} \cdot \text{m}^2$, $v_{\text{mol}} = 3140.9(1) \text{ \AA}^3$, and $s_{\text{mol}} = 3031.2(1) \text{ \AA}^2$. From these data, it may be concluded that the crystal is made from the stacking of oblate-shaped symmetric tops ($1.23 \times 1.06 \times 1.06 \text{ nm}$) characterized by a compactness factor of about 40.6%. One may also notice in this highly symmetrical species a small cavity located at the center of the cluster. As already quoted at that time by Achim himself: *No significant residual*

electron density could be located inside the cavity. The question of whether possibly “water” is present in the cavity, cannot be answered conclusively... For such “porous” structures a further computable property should be the internal van der Waals radius R_{int} , corresponding to the largest sphere making no contact with surrounding atoms. For this cluster we got an inscribed radius $R_{\text{int}} = 2.11 \text{ \AA}$, corresponding to an accessible free volume of only 39 \AA^3 . By comparison using the same set of radii, a single water molecule is characterized by: $R_{\text{ext}} = 2.01 \text{ \AA}$ (bulk volume 34 \AA^3), $\rho = 0.878 \text{ g} \cdot \text{cm}^{-3}$, $I_A = 29.4 \times 10^{-46} \text{ kg} \cdot \text{m}^2$, $I_B = 19.2 \times 10^{-46} \text{ kg} \cdot \text{m}^2$, $I_C = 10.2 \times 10^{-46} \text{ kg} \cdot \text{m}^2$, $v_{\text{mol}} = 18.8(1) \text{ \AA}^3$, and $s_{\text{mol}} = 35.0(1) \text{ \AA}^2$. These data clearly show that there is room enough for just one water molecule inside this kind of cavity. Single isolated water molecules forming no hydrogen bonds with other water molecules being very rare in aqueous solutions, we may safely assume that this cavity is really empty.

So far for the central cavity, but an interesting observation is nevertheless that quite a large difference is observed between the density of the cluster ($\rho = 1.975 \text{ g} \cdot \text{cm}^{-3}$) and that of the whole crystal calculated from X-ray diffraction data ($\rho = 2.67 \text{ g} \cdot \text{cm}^{-3}$) [5]. Obviously, this means that the $\text{Mo}_{57}\text{Fe}_6$ cluster cannot be the whole story in this kind of compound and that a significant amount of matter is sitting just outside, probably filling the interstices generated by the packing of these non-spherical polyanionic units. At this stage, it is time to have a look at what is usually neglected during crystal structure analysis, viz. the poor solvent molecules squeezed between the most massive eye-catching molecular components.

A first way to start this hunt for water clusters buried in crystalline structures is to choose a fixed threshold for $\text{O} \cdots \text{O}$ and $\text{N} \cdots \text{O}$ distances above which H-bond formation is expected not to occur. Then, using a convolute sphere search based on this radius around each O-atom or N-atom not belonging to the $\text{Mo}_{57}\text{Fe}_6$ polyanion, one may seek for non-diverging solutions. An easy and quick way to select these “isolated” atoms from a CIF file that may contain several hundred atomic positions is to rely on the bond valence sum technique [25]. Bond valence sums less than one for a nitrogen or an oxygen atom is a very sensitive test for missing H-atoms around these elements. In the present case, ammonium atoms were found to be labeled N2, N3, N5, free water molecules O27, O29–O32, O34–O39 and water molecules bonded to sodium ions O26, O28, and O33. All other atoms of the structure are bonded either to Mo or Fe and were thus discarded from the search runs. Once a cluster has been identified, H-atoms are arbitrarily added assuming typical O–H and N–H bond lengths of 97 and 103 pm respectively, and typical bond angles: $\theta_{\text{H-O-H}} = 105^\circ$ and $\theta_{\text{H-N-H}} = 109.5^\circ$. The basic idea is to vary H-atoms coordinates randomly in such a way that each O-atom or N-atom is always

surrounded by two (oxygen) or four (nitrogen) H-atoms spanning the vertices of a V-shaped molecule (water) or those of a regular tetrahedron (ammonium). For each shot the electrostatic part (named $\langle EB \rangle$ hereafter) of the total molecular energy is computed and the variation is stopped when some converging criterion is satisfied (typically variations of $\langle EB \rangle$ less than 10^{-6}). At that point we have to stress that we entirely rely on the amazing capability of Achim's group to make a clear distinction between water molecules and ammonium ions in a single-crystal X-ray diffraction experiment. As this distinction is not an obvious and trivial task, it follows that the existence of mixed clusters based on ammonium and water molecules, if strongly suggested, is by no means proved. The following results should then be taken "as such" and we have to wait for decisive NMR experiments on these phases to confirm or infirm the existence of these mixed clusters.

As a first example of this procedure let's consider the largest cluster (eighteen O-atoms) found in this structure by looking around atoms O36 or O39 with a threshold of 300 pm. After dressing this naked oxygen cluster with its H-atoms suit, we got after energy minimization the very beautiful crown of eighteen-water molecules displayed at the bottom of Fig. 2. Obviously, it is a little bit amazing that such a beautiful supramolecule was sleeping there unnoticed for about ten years, quietly waiting for Achim's 65th birthday. From an energetic standpoint this crown is characterized by $\langle EB_{\text{crown}} \rangle = -3620.0 \text{ kJ} \cdot \text{mol}^{-1}$. By comparison with the electrostatic balances of 18 free water molecules ($\langle EB_{\text{wat}} \rangle = -171.252 \text{ kJ} \cdot \text{mol}^{-1}$ for each), we estimate a mean H-bond energy $\langle E_{\text{HB}} \rangle = (-3620.0 + 18 \times 171.25) / 18 = -29.9 \text{ kJ} \cdot \text{mol}^{-1}$, a value typical of Achim's water clusters (H-bonds stronger than in crystalline ices). Concerning the molecular size of this object we found: $R_{\text{ext}} = 7.94 \text{ \AA}$, $\rho = 0.257 \text{ g} \cdot \text{cm}^{-3}$ (15.4% compactness), $I_A = 13.5 \times 10^{-42} \text{ kg} \cdot \text{m}^2$, $I_B = 76.8 \times 10^{-42} \text{ kg} \cdot \text{m}^2$, $I_C = 76.5 \times 10^{-42} \text{ kg} \cdot \text{m}^2$ (oblate symmetric top), $v_{\text{mol}} = 322.1(5) \text{ \AA}^3$ and $s_{\text{mol}} = 456.2(5) \text{ \AA}^2$. Let's also notice that the tricky aspect of the left drawing in Fig. 2, showing a large central cavity at the center of the crown. As shown in other drawings this cavity is in fact an illusion, as a quantitative evaluation leads to $R_{\text{int}} = 1.79 \text{ \AA}$, corresponding to an accessible volume of only 24 \AA^3 . This example clearly shows that water molecules are able to associate themselves into quite tortuous supramolecular architectures.

Let's now review some smaller water-based jewels also contained in this amazing casket. The top left drawing of Fig. 3 shows a very strange cationic species $[(\text{NH}_4)_3(\text{H}_2\text{O})_8]^{3+}$ characterized by: $R_{\text{ext}} = 8.29 \text{ \AA}$, $\rho = 0.138 \text{ g} \cdot \text{cm}^{-3}$ (9.2% compactness), $I_A = 49.7 \times 10^{-43} \text{ kg} \cdot \text{m}^2$, $I_B = 30.3 \times 10^{-43} \text{ kg} \cdot \text{m}^2$, $I_C = 29.3 \times 10^{-43} \text{ kg} \cdot \text{m}^2$ (asymmetric top), $v_{\text{mol}} = 220.2(4) \text{ \AA}^3$, $s_{\text{mol}} = 366.0(0) \text{ \AA}^2$, and $\langle EB_{\text{AM3W8}} \rangle = -1995.0 \text{ kJ} \cdot \text{mol}^{-1}$. It was found by looking around N3

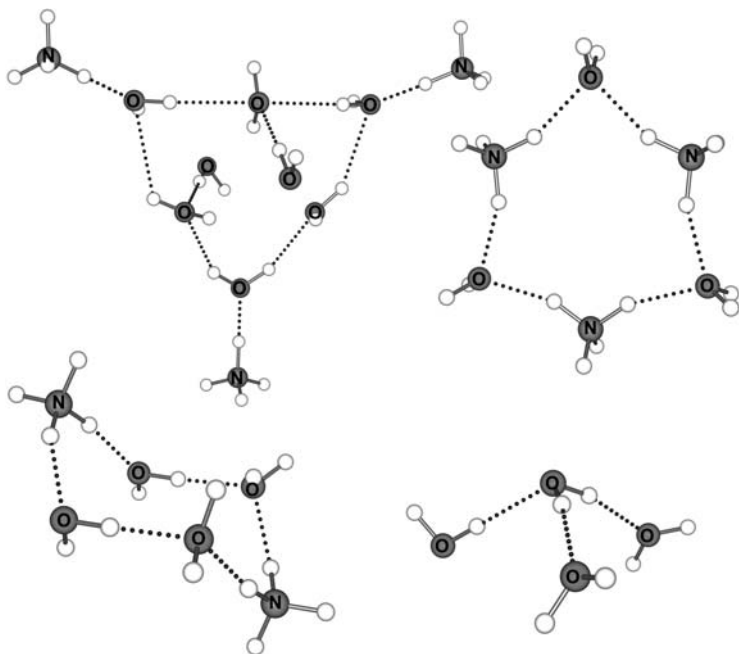


Fig. 3. Some water-based aggregates sitting between the stacking of $[\text{Mo}_{57}\text{Fe}_6(\text{NO})_6\text{O}_{174}(\text{OH})_3(\text{H}_2\text{O})_{24}]$ clusters. Top left: a $[(\text{NH}_4)_3(\text{H}_2\text{O})_8]^{3+}$ cluster built from three strongly solvated $[(\text{NH}_4)(\text{H}_2\text{O})]^+$ units weakly associated by 2 water dimers and one water monomer. Top right: a perfectly planar $[(\text{NH}_4)_3(\text{H}_2\text{O})_3]^{3+}$ hexagon. Bottom left: a chair-shaped $[(\text{NH}_4)_2(\text{H}_2\text{O})_4]^{2+}$ hexagon. Bottom right: a triangular pyramidal water tetramer $[\text{H}_2\text{O}]_4$.

with a radius of 320 pm and involves in its structure besides N3, atoms O27, O34, and O35. Let's analyze in fine details the building scheme of this interesting nano-object. After removal of the three ammonium cations, we are left with a eight-member water cluster characterized by $\langle EB_{\text{w}8} \rangle = -1478.4 \text{ kJ} \cdot \text{mol}^{-1}$. By reference with the electrostatic balance of three isolated ammonium ions ($\langle EB_{\text{AM}} \rangle = -127.74 \text{ kJ} \cdot \text{mol}^{-1}$), we got a mean H-bond energy $\langle E_{\text{HB}} \rangle = (-1995.0 + 3 \times 127.74)/3 = -44.5 \text{ kJ} \cdot \text{mol}^{-1}$. This is an amazingly strong value, obviously associated with the very short $\text{O} \cdots \text{N}$ distance (257 pm) and perfectly linear $\text{N}-\text{H} \cdots \text{O}$ bridge ($q_{\text{H-N} \cdots \text{O}} < 1^\circ$). On the other hand, if we remove the two outer water molecules not belonging to the $(\text{H}_2\text{O})_6$ ring, we got a cluster characterized by $\langle EB_{\text{AM}3\text{W}6} \rangle = -1598.8 \text{ kJ} \cdot \text{mol}^{-1}$. The mean energy of association with the ring for these two water molecules ($d_{\text{O} \cdots \text{O}} = 300 \text{ pm}$ and $\theta_{\text{H-O} \cdots \text{O}} < 5^\circ$) is thus $\langle E_{\text{HB}} \rangle = (-1995.0 + 1598.8 + 2 \times 171.25)/2 = -26.9 \text{ kJ} \cdot \text{mol}^{-1}$, a value commonly encountered in crystalline ices. At last, we may evaluate the

association energy within the ring itself characterized by $\langle EB_{w6} \rangle = -1086.9 \text{ kJ} \cdot \text{mol}^{-1}$, leading to $\langle E_{\text{HB}} \rangle = (-1086.9 + 6 \times 171.25)/6 = -9.9 \text{ kJ} \cdot \text{mol}^{-1}$. This pretty low value is obviously linked to the quite long $\text{O} \cdots \text{O}$ distance (319 pm) associated to large deviations from linearity ($\text{H}-\text{O} \cdots \text{O}$ angles ranging from 14 up to 42°). With these data in hand, the structure of this cluster is no more surprising, as it may be seen as a rather loose association of three strongly solvated ammonium ions $[\text{H}_3\text{N}-\text{H} \cdots \text{OH}_2]^+$ mediated by two water dimers and one water molecule. This second example thus provides us with a clear structural example of the kind of association that may exist between ammonium ions and water molecules. It raises also the question of the possible existence of mixed copolymers based on hydrogen bridges involving both ammonium ions and water molecules.

The top right drawing of Fig. 3 brings a first appealing answer to this question. Accordingly, by looking around atom N2 with a threshold of 320 pm, we got a perfectly planar mixed six-member ring based on three ammonium ions (atomic site N2) and three water molecules (atomic site O32). This highly symmetric cation is characterized by: $R_{\text{ext}} = 4.99 \text{ \AA}$, $\rho = 0.345 \text{ g} \cdot \text{cm}^{-3}$ (24.1% compactness), $I_A = 14.6 \times 10^{-43} \text{ kg} \cdot \text{m}^2$, $I_B = I_C = 74.1 \times 10^{-43} \text{ kg} \cdot \text{m}^2$ (oblate symmetric top), $v_{\text{mol}} = 125.8(3) \text{ \AA}^3$, $s_{\text{mol}} = 216.5(4) \text{ \AA}^2$, and $\langle EB_{\text{AM}3\text{W}3} \rangle = -1006.8 \text{ kJ} \cdot \text{mol}^{-1}$. With six hydrogen bonds, the mean H-bond energy in this ring is readily evaluated as $\langle E_{\text{HB}} \rangle = [-1006.8 + 3 \times (127.74 + 171.25)]/6 = -18.3 \text{ kJ} \cdot \text{mol}^{-1}$ ($d_{\text{O} \cdots \text{N}} = 281 \text{ pm}$ and $\theta_{\text{H}-\text{N}-\text{O}} = 13^\circ$). One thus observe that changing from a terminal to a bridging position for ammonium ions in water-based rings leads to about one half reduction in H-bond strength. Interestingly enough, another kind of six-member ring built from two ammonium ions and four water molecules (atomic site O38) may be found by lurking around atom N5 with a threshold of 320 pm. As shown in the bottom left part of Fig. 3, replacing an ammonium ion by a water molecule leads to a puckered chair-shaped hexagonal ring, quite similar to that found in ice I_h . This mixed chair is characterized by: $R_{\text{ext}} = 5.17 \text{ \AA}$, $\rho = 0.311 \text{ g} \cdot \text{cm}^{-3}$ (20.5% compactness), $I_A = 11.2 \times 10^{-43} \text{ kg} \cdot \text{m}^2$, $I_B = 78.8 \times 10^{-43} \text{ kg} \cdot \text{m}^2$, $I_C = 49.1 \times 10^{-43} \text{ kg} \cdot \text{m}^2$ (asymmetric top), $v_{\text{mol}} = 118.8(3) \text{ \AA}^3$, $s_{\text{mol}} = 181.8(3) \text{ \AA}^2$, and $\langle EB_{\text{AM}2\text{W}4} \rangle = -1081.5 \text{ kJ} \cdot \text{mol}^{-1}$. After removal of the two ammonium ions we got two pairs of dimers characterized by $\langle EBW_4 \rangle = -747.8 \text{ kJ} \cdot \text{mol}^{-1}$. The binding energy of these ions to the ring is then evaluated as $\langle E_{\text{HB}} \rangle = [-1081.5 + 2 \times 127.74 + 747.8]/4 = -19.6 \text{ kJ} \cdot \text{mol}^{-1}$. This value is consistent with the previous one derived from a quite similar bridging position for ammonium species. The slight decrease in energy may be related to the smaller distance: 279 pm for the $[(\text{NH}_4)_2(\text{H}_2\text{O})_4]^{2+}$ ion versus 281 pm for the $[(\text{NH}_4)_3(\text{H}_2\text{O})_3]^{2+}$ ion. One may also notice the larger spreading of

H-N...O angles for the di-ammonium ring ($8^\circ < \theta < 21^\circ$) relative to the tri-ammonium case (all angles at 13°). Let's also notice that if both rings are very close from a H-bond strength viewpoint, they nevertheless differ from the compactness standpoint. The planar ring offers a much larger central cavity ($R_{\text{int}} = 0.94 \text{ \AA}$, corresponding of an accessible volume of 3.5 \AA^3) than the puckered one ($R_{\text{int}} = 0.62 \text{ \AA}$, corresponding to an accessible volume of only 1.0 \AA^3).

At this stage we are left will only atoms O29–O31 and O37 that remain yet unvisited. On may then expect the existence of some smaller pure water clusters based on these atoms. This was found to be the case as two water tetramers were found by creeping around O29 or O37 with a 320 pm threshold. The bottom right part of Fig. 3 shows the two triangular pyramidal geometry observed for these two species. If these two tetramers display exactly the same H-bond topology, they nevertheless differ from a metrical standpoint. The tetramer based on atomic sites O29 and O31 is characterized by: $R_{\text{ext}} = 4.99 \text{ \AA}$, $\rho = 0.230 \text{ g} \cdot \text{cm}^{-3}$ (14.1% compactness), $I_A = 5.4 \times 10^{-43} \text{ kg} \cdot \text{m}^2$, $I_B = 3.2 \times 10^{-43} \text{ kg} \cdot \text{m}^2$, $I_C = 3.1 \times 10^{-43} \text{ kg} \cdot \text{m}^2$ (oblate symmetric top), $v_{\text{mol}} = 73.2(2) \text{ \AA}^3$, $s_{\text{mol}} = 114.4(2) \text{ \AA}^2$ and $\langle EB_{\text{W4A}} \rangle = -783.1 \text{ kJ} \cdot \text{mol}^{-1}$. With such a structure, it is possible to probe the energetic difference between an acceptor situation $\text{HO}-\text{H} \cdots \text{OH}_2(\text{H}_2\text{O})_2$ and a donor one $\text{H}_2\text{O} \cdots \text{H}-\text{O}-\text{H} \cdots \text{OH}_2$ for the central atom. When we remove the left donor water molecule, we are left with a trimer characterized by $\langle EB_{\text{W3A}} \rangle = -579.5 \text{ kJ} \cdot \text{mol}^{-1}$ and forming two donor-type H-bonds. It then follows that for a donor geometry at $d_{\text{O} \cdots \text{O}} = 275 \text{ pm}$, we have: $\langle E_{\text{HB}} \rangle(\text{donor}) = [-579.5 + 3 \times 171.25]/2 = -32.9 \text{ kJ} \cdot \text{mol}^{-1}$. If on the other hand, we remove from the tetramer the two right-sided acceptors, we are left with a dimer characterized by $\langle EB_{\text{W2A}} \rangle = -372.0 \text{ kJ} \cdot \text{mol}^{-1}$ and forming one acceptor-type H-bond. For exactly the same O...O distance we thus found $\langle E_{\text{HB}} \rangle(\text{acceptor}) = (-372.0 + 2 \times 171.25) = -29.5 \text{ kJ} \cdot \text{mol}^{-1}$. For the other tetramer based on atomic sites O37 and O30 we got: $R_{\text{ext}} = 5.13 \text{ \AA}$, $\rho = 0.212 \text{ g} \cdot \text{cm}^{-3}$ (6.4% compactness), $I_A = 6.6 \times 10^{-43} \text{ kg} \cdot \text{m}^2$, $I_B = 3.8 \times 10^{-43} \text{ kg} \cdot \text{m}^2$, $I_C = 3.7 \times 10^{-43} \text{ kg} \cdot \text{m}^2$ (oblate symmetric top), $v_{\text{mol}} = 75.0(2) \text{ \AA}^3$, $s_{\text{mol}} = 115.5(3) \text{ \AA}^2$, and $\langle EB_{\text{W4B}} \rangle = -752.8 \text{ kJ} \cdot \text{mol}^{-1}$. Proceeding as before for the evaluation of the donor versus acceptor H-bond strength leads to $\langle EB_{\text{W3B}} \rangle = -558.5 \text{ kJ} \cdot \text{mol}^{-1}$, i.e., to $\langle E_{\text{HB}} \rangle(\text{donor}) = [-558.5 + 3 \times 171.25]/2 = -22.4 \text{ kJ} \cdot \text{mol}^{-1}$ and to $\langle EB_{\text{W2B}} \rangle = -363.2 \text{ kJ} \cdot \text{mol}^{-1}$, i.e., to $\langle E_{\text{HB}} \rangle(\text{acceptor}) = [-363.2 + 2 \times 171.25]/2 = -20.7 \text{ kJ} \cdot \text{mol}^{-1}$. The large difference in H-bond strength between the two tetramers is easily explained by the significantly higher O...O distance (300 pm) in the second cluster. It then remains that in both cases we found, as expected, an acceptor geometry less stable than the donor one. An interesting point is that this occurs despite a better linearity observed for

the hydrogen bridge in the acceptor case ($\theta_{\text{H-O}\cdots\text{O}} = 2^\circ$ and 0° for A and B respectively) relative to the donor case ($\theta_{\text{H-O}\cdots\text{O}} = 8^\circ$ for both A and B). Here, it is clear that the factor favoring the donor geometry lies in the fact that two favorable $\delta^+ \cdots \delta^-$ interactions (against only one for the acceptor geometry) exists between the central O-atom and the two H-atoms located on the other H-bonded O-atom.

Having finished the inventory of our jewelry, it is now time to ask if such species are really independent from each other, or if they may be further associated together in the solid state to form supramolecular chains or layers. Figure 4 shows the wonderful 2D-layer that can be formed using the $(\text{H}_2\text{O})_{18}$ crown, the $[(\text{NH}_4)_2(\text{H}_2\text{O})_4]^{2+}$ chair-shaped hexagon and one of the water molecule (O33) belonging to the coordination sphere of the sodium atom. Without this last water molecule, the crown and the chair would have formed isolated entities. If one has already wondered what should be the structure of an aqueous solution containing ammonium ions in the vicinity of a polyelectrolyte (a protein for instance), we get here a possible quite realistic picture. We really think that this direct visualization of the structure of aqueous solutions near charged interfaces is one of the several fascinating applications of Achim's research. Figure 4 also shows that large voids formed by 15-member rings occur in this layer. In fact, these voids are far from being empty, the two types of $(\text{H}_2\text{O})_4$ tetramers filling these in conjunction with Na^+ cations. The two remaining isolated clusters, $[(\text{NH}_4)_3(\text{H}_2\text{O})_8]^{3+}$ and $[(\text{NH}_4)_3(\text{H}_2\text{O})_3]^{3+}$ are found not to be

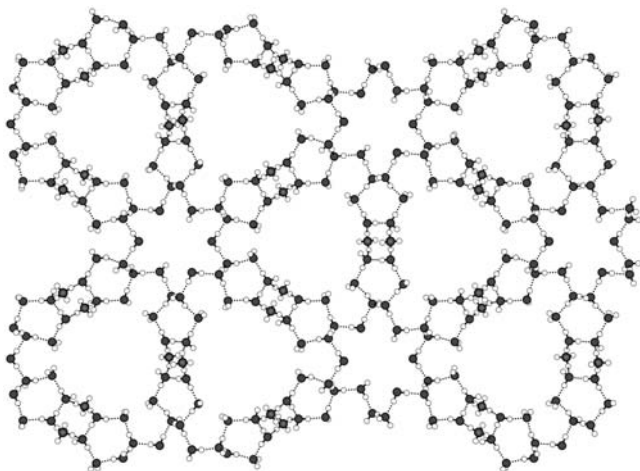


Fig. 4. The 2-D layer formed by the association through a water molecule (O33) of crowns $(\text{H}_2\text{O})_{18}$ and chair-shaped hexagons $[(\text{NH}_4)_2(\text{H}_2\text{O})_4]^{2+}$.

involved in these layers but are just trapped in sandwich position between two successive layers leading to a 3D-network.

THE $(\text{H}_2\text{O})_{100}$ CLUSTER

This cluster was characterized by X-ray diffraction after reaction between $(\text{NH}_4)_{42}[\text{Mo}_{132}\text{O}_{372}(\text{H}_2\text{O})_{72}(\text{H}_2\text{PO}_2)_{30}] \cdot n\text{H}_2\text{O}$ ($n \sim 300$) and guanidinium sulfate leading to the compound $(\text{gua})_{32}[\text{Mo}_{132}\text{O}_{372}(\text{H}_2\text{O})_{72}(\text{SO}_4)_{10}(\text{H}_2\text{PO}_2)_{20}(\text{gua})_{20}] \cdot n\text{H}_2\text{O}$ ($n \sim 200$) ($\text{gua} = [(\text{NH}_2)_3\text{C}]^+$) [21]. In contrast with the previous case, we have here an example of a cavity large enough to hold a great amount of water molecules (Fig. 5 top). The

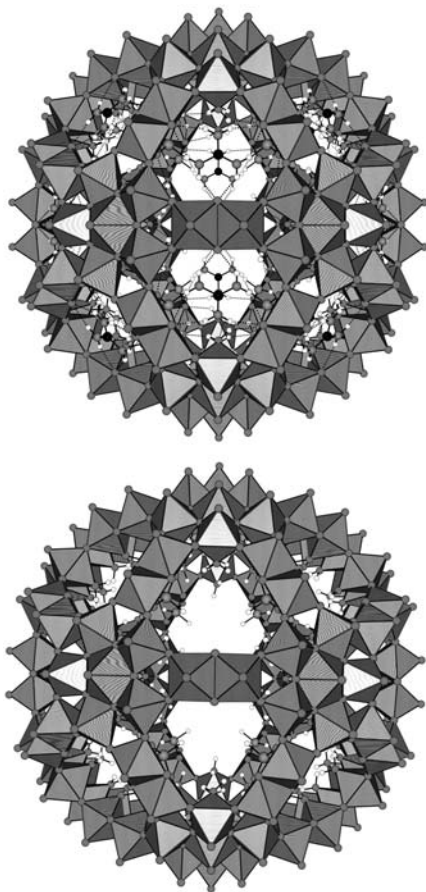


Fig. 5. The full (top) and empty (bottom) perforated nanocapsule acting as a container of the well-organized $(\text{H}_2\text{O})_{100}$ water cluster.

bottom drawing of Fig. 5 shows the structure of an empty ball displaying a $[\text{Mo}_{132}\text{O}_{372}(\text{H}_2\text{O})_{72}(\text{H}_2\text{PO}_2)_{30}]$ stoichiometry. Let's notice that the presence of some sulfate ions is absolutely necessary for stabilizing the central $(\text{H}_2\text{O})_{100}$ cluster. However, only phosphorus atoms were present in the CIF file provided with the published structure [21]. Similarly to the water/ammonium case, this probably reflects the difficulty to distinguish between hypophosphite and sulfate ions from single-crystal X-ray diffraction data alone. After several unsuccessful trials for modeling a $\text{SO}_4/\text{H}_2\text{PO}_2$ ratio equal to 10/20, we have decided to use the X-ray data "as provided" without any sulfate ions. If this point is of minor importance for the empty capsule or for the water cluster isolated from its container, this is no more the case for the real water-filled capsule. Consequently, results on the water-filled capsule should be considered only as preliminary results subjected to changes, when better structural data would become available.

Geometrical characteristics of the $[\text{Mo}_{132}\text{O}_{372}(\text{H}_2\text{O})_{72}(\text{H}_2\text{PO}_2)_{30}]$ perforated nanocapsule are found to be: $R_{\text{ext}} = 16.46 \text{ \AA}$, $\rho = 1.944 \text{ g}\cdot\text{cm}^{-3}$ (44.0% compactness), $I_A = 41.1 \times 10^{-40} \text{ kg}\cdot\text{m}^2$, $I_B = 40.8 \times 10^{-40} \text{ kg}\cdot\text{m}^2$, $I_C = 40.8 \times 10^{-40} \text{ kg}\cdot\text{m}^2$ (spherical top), $v_{\text{mol}} = 8222(3) \text{ \AA}^3$, $s_{\text{mol}} = 8147(2) \text{ \AA}^2$, and $\langle EB_{\text{cap}} \rangle = -499338.5 \text{ kJ}\cdot\text{mol}^{-1}$. Concerning the central cavity, it is characterized by $R_{\text{int}} = 7.56 \text{ \AA}$, corresponding to an accessible volume of 1810 \AA^3 . Even if completely empty, it may be of some interest to have a look at the intramolecular possibilities of hydrogen bonding involving water molecules bonded to Mo-atom either in a central pentagonal bipyramid, or in the five octahedra sharing edges with this central hepta-coordinated unit. Figure 6 (left) shows the kind of geometry encountered for the twelve $\{\text{Mo}[\text{D}_{5h}]\}\{\text{Mo}[\text{O}_h]\}_5$ groups acting as building units of the Mo_{132} nanocapsule. It is found that the central water molecule belonging to the sevenfold coordinated Mo-atom acts as a double donor towards two water molecules located on one chord of the pentagon. It also acts as a double acceptor towards two other water molecules located on a chord at right angle from the first one. The water molecule on the last vertex is not H-bonded to the five others, but may form nevertheless another intramolecular bridge with one O-atom of a neighboring hypophosphite group linking together two MoO_6 octahedra (Fig. 6 right). In contrast, the other O-atom of this hypophosphite bridge forms two H-bonds with two water molecules of a neighboring $\{\text{Mo}[\text{D}_{5h}]\}\{\text{Mo}[\text{O}_h]\}_5$ unit. Repetition of this H-bonding scheme along the twelve Mo_6 units and along the thirty Mo_2 units, thus defines a nice web of 138 hydrogen bonds covering the internal face of the cavity. Let's notice that, as expected, the sixty H-P bonds do not form any hydrogen bonds.

Let's now turn our attention towards the hydrogen bond system involving the guanidinium ions. As shown in Fig. 5 (bottom), each cation

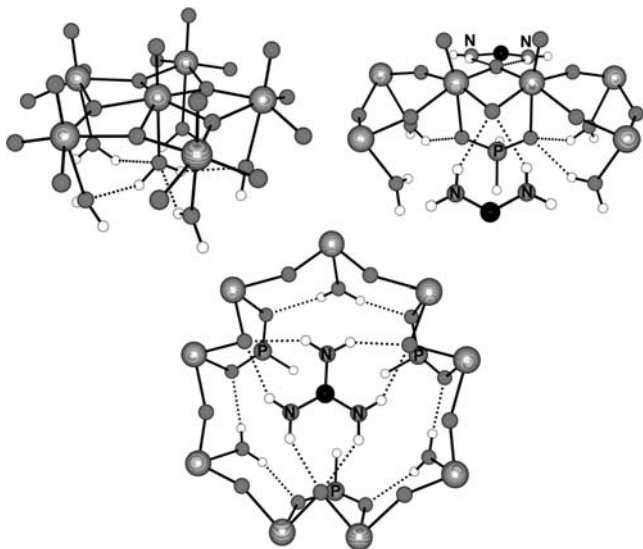


Fig. 6. The intramolecular H-bond patterns characterizing the $[\text{Mo}_{132}\text{O}_{372}(\text{H}_2\text{O})_{72}(\text{H}_2\text{PO}_2)_{30}\{\text{C}(\text{NH}_2)_3\}_{20}]$ nanocapsule. Top left: hydrogen bonding within the $\{\text{Mo}[\text{D}_{5h}]\}\{\text{Mo}[\text{O}_h]\}_5$ building units. Top right: hydrogen bonding with hypophospite groups and edge-sharing MoO_6 octahedra. Bottom: hydrogen bonding between guanidinium cations and the three μ_2 -oxo groups defining the nine-member pore ring.

is involved in a very symmetric fashion into six H-bonds with three μ_2 -oxo groups belonging to three edge-sharing octahedral Mo_2 units. The figure also shows part of the previously discussed underlying web involving $\text{Mo}-\text{OH}_2$ water molecules and $[\text{H}_2\text{PO}_2]^-$ anions. In order to quantify the energy of interaction of these cations with these nine-member pore rings, we just have to evaluate the electrostatic balance of a system displaying a $[\text{Mo}_{132}\text{O}_{372}(\text{H}_2\text{O})_{72}(\text{H}_2\text{PO}_2)_{30}\{\text{C}(\text{NH}_2)_3\}_{20}]$ stoichiometry ($\langle EB_{\text{guacap}} \rangle = -509954.4 \text{ kJ}\cdot\text{mol}^{-1}$) and that corresponding to the sum of twenty free guanidinium cations ($\langle EB_{\text{gua20}} \rangle = -10049.2 \text{ kJ}\cdot\text{mol}^{-1}$). Consequently, for this system of 120 equivalent H-bonds we got a total interaction energy $\langle EB_{\text{guacap}} \rangle - (\langle EB_{\text{gua20}} \rangle + \langle EB_{\text{cap}} \rangle) = -566.7 \text{ kJ}\cdot\text{mol}^{-1}$, corresponding to a mean H-bond energy $\langle E_{\text{HB}}(\text{gua}) \rangle = -4.7 \text{ kJ}\cdot\text{mol}^{-1}$. This is a pretty low value relative to other H-bonds encountered in this study, obviously related to the fact that we have used H-atom coordinates provided by X-ray diffraction leading to unrealistically short N-H distances (all less than 90 pm). Increasing this distance up to 103 pm as in the previous case would lead to a corresponding shortening of the N-H...O distance and thus to a much more stable hydrogen bridge (about $-10 \text{ kJ}\cdot\text{mol}^{-1}$).

After this discussion of all the possible intramolecular H-bonds in this nanocapsule, we may have a look at the most interesting piece: the $(\text{H}_2\text{O})_{100}$ cluster. Water molecules in this $(\text{H}_2\text{O})_{100}$ cluster (Figs. 7 and 8) are highly organized with three concentric shells having radii of 3.84–4.04, 6.51–6.83, and 7.56–7.88 Å and spanned by 20, 20, and 60 molecules, respectively. This structure may be described as a central dodecahedron of water molecules (twelve five-member rings) with its 20 vertices decorated by a water molecule and encapsulated into a rhombicosidodecahedron of water molecules (boat-shaped six-member rings). Interestingly enough, exactly the same arrangement was found to occur as the central core of a $(\text{H}_2\text{O})_{280}$ cluster obtained after molecular dynamics calculations [26]. However, before analyzing this cluster in terms of H-bond strengths, one may wonder why it is so well organized with absolutely no disorder detected by X-ray diffraction. Accordingly, X-ray diffraction shows that some of the guanidinium ions are stuck onto the twenty larger pores and cannot penetrate inside the cavity (cf. Figs. 5 and 6). The inwards osmotic pressure Π generated by these cations unable to enter the cavity may then be roughly estimated as $\Pi(\text{kPa}) = R \times \Delta c(\text{mol} \cdot \text{l}^{-1}) \times T(\text{K})$, where R is the perfect gas constant ($8,315 \text{ J} \cdot \text{mol}^{-1} \cdot \text{K}^{-1}$) and Δc the difference in concentration between both sides. If n_{in} and n_{out} stands for the number of species found respectively inside and outside a volume V , we may write: $\Delta c(\text{mol} \cdot \text{l}^{-1}) \sim 1.66 \times |n_{\text{in}} - n_{\text{out}}| / V(\text{nm}^{-3})$. In our case, 20 guanidinium cations are excluded from a central water droplet offering a volume of 4.354 nm^3 , leading to $\Delta c \sim 7.6 \text{ mol} \cdot \text{l}^{-1}$ ($n_{\text{in}} = 0$ and $n_{\text{out}} = 20$) and with $T = 300 \text{ K}$ to $\Pi \sim 19 \text{ MPa}$ (about 190 bar, i.e., the pressure at a sea-depth of 1900 m). This value is well below the pressure needed for the appearance of eight-member rings occurring in the ice-II structure and in other high-pressure polymorphs ($P > 100 \text{ MPa}$). On the other hand it is quite similar to that needed to form clathrate hydrates structures based on the pentagonal dodecahedron. The overall result of this entropy-driven process is the wonderful dodecahedron $(\text{H}_2\text{O})_{20}$ inscribed inside the central cavity.

In a first pass, we have considered the whole system made of a $[\text{Mo}_{132}\text{O}_{372}(\text{H}_2\text{O})_{72}(\text{H}_2\text{PO}_2)_{30}\{\text{C}(\text{NH}_2)_3\}_{20}]$ capsule filled by one hundred water molecules (Fig. 5 top). At this stage, it has to be noticed that this is quite a “big” system made of 1370 atoms, displaying a molecular weight of $24867.22 \text{ g} \cdot \text{mol}^{-1}$ and defining a 372-D hypersurface onto which we have to move H-atoms in order to find an energetic minimum. With such a system, we are at the very limit of our present computing capabilities, but the problem remains nevertheless tractable on a single processor machine, providing that we allow the system to run exclusively during at least one week (for a pentium-4 cadenced at 2 GHz machine). The consequence of this matter of fact is that the probability of landing into a local minimum is

pretty high and thus the following results concerning the encapsulated water cluster should not be considered as definitive. They are presented at the current level of convergence ($\langle EB_{\text{tot}} \rangle = -531418.3 \text{ kJ} \cdot \text{mol}^{-1}$) and are thus subject to minor quantitative changes in the very next future.

The bottom drawing of Fig. 7 shows the geometry of the encapsulated cluster characterized by: $R_{\text{ext}} = 10.19 \text{ \AA}$, $\rho = 0.675 \text{ g} \cdot \text{cm}^{-3}$ (37.7% compactness), $I_A = 96.8 \times 10^{-42} \text{ kg} \cdot \text{m}^2$, $I_B = 95.5 \times 10^{-42} \text{ kg} \cdot \text{m}^2$, $I_C = 95.4 \times 10^{-42} \text{ kg} \cdot \text{m}^2$ (spherical top), $v_{\text{mol}} = 1669(1) \text{ \AA}^3$, $s_{\text{mol}} = 1948(2) \text{ \AA}^2$, and $\langle EB_{\text{W100I}} \rangle = -21069.6 \text{ kJ} \cdot \text{mol}^{-1}$. The filling factor of the cavity is then evaluated as $f = 1669 \times 100 / 1810 = 92\%$, showing that very little room is left between

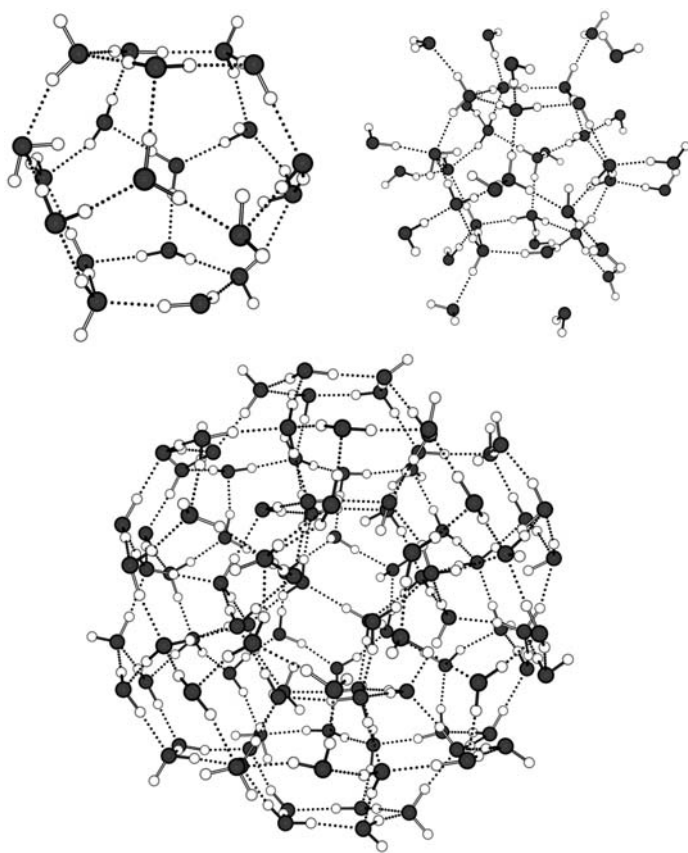


Fig. 7. The $(\text{H}_2\text{O})_{100}$ water cluster trapped inside the $[\text{Mo}_{132}\text{O}_{372}(\text{H}_2\text{O})_{72}(\text{SO}_4)_{10}(\text{H}_2\text{PO}_2)_{20}(\text{gua})_{20}]$ nanocapsule. Top left: the central $(\text{H}_2\text{O})_{20}$ dodecahedron displaying 29 intramolecular hydrogen bonds. Top right: the vertex-decorated $(\text{H}_2\text{O})_{40}$ dodecahedron with some non-bonded water molecules. Bottom: the full cluster with its 163 intramolecular hydrogen bonds.

the outer tips of the cluster and the cavity walls. A clue showing that we are not yet fully converged is that we expect a system of 170 intramolecular H-bonds and that we observe only 163 of them. Figure 8 shows the histograms obtained in this cluster for the two fundamental quantities characterizing any H-bonded system: the H–O···O non-bonded angle and the O–H···O energy of interaction. The wiggles observed for the largest angles and the occurrence of positive values for the H-bond energy are direct proofs that a better solution, lower in energy, should exist. Besides this characterization on a per-H-bond basis, we may be interested by interaction energies in supramolecular assemblies. The top left drawing of Fig. 7 shows the geometry observed for the central dodecahedron made of twenty water molecules. With $\langle EB_{W20I} \rangle = -3969.5 \text{ kJ} \cdot \text{mol}^{-1}$ corresponding to a total of 29 hydrogen bonds, we get $\langle E_{HB} \rangle = (\langle EB_{W20I} \rangle + 20 \times 171.25) / 29 = -18.8 \text{ kJ} \cdot \text{mol}^{-1}$. If we add the twenty other water molecules onto each vertex (top right of Fig. 7), we get a $(\text{H}_2\text{O})_{40}$ water cluster characterized by

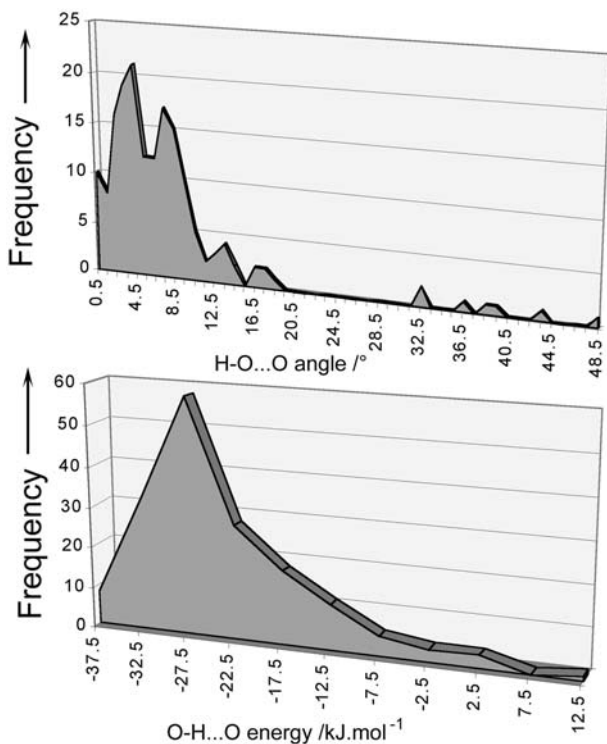


Fig. 8. Angular ($\theta_{\text{H-O}\cdots\text{O}}$) distribution function (top) for the H-bond pattern found in the encapsulated $(\text{H}_2\text{O})_{100}$ cluster and its associates energetic partition function (bottom).

$\langle EB_{W40I} \rangle = -7903.6 \text{ kJ} \cdot \text{mol}^{-1}$ and 47 H-bonds. Again, the occurrence of some water molecules not bonded with the central dodecahedron is indicative of a non-converged solution. The interaction energy associated to this vertex sharing addition is then $\langle E_{HB} \rangle = (\langle EB_{W40I} \rangle + \langle EB_{W20I} \rangle + 20 \times 171.25) / 18 = -28.3 \text{ kJ} \cdot \text{mol}^{-1}$. There is thus a clear anisotropy of the H-bond energy in this system. Finally, capping this entity by the sixty remaining water molecules (bottom of Fig. 7) corresponds to a mean H-bond energy evaluated as $\langle E_{HB} \rangle = (\langle EB_{W100I} \rangle + \langle EB_{W40I} \rangle + 60 \times 171.25) / 116 = -24.9 \text{ kJ} \cdot \text{mol}^{-1}$. As expected, this is an intermediate value corresponding to the fact that new pentagonal faces are created and that further vertex sharing is occurring.

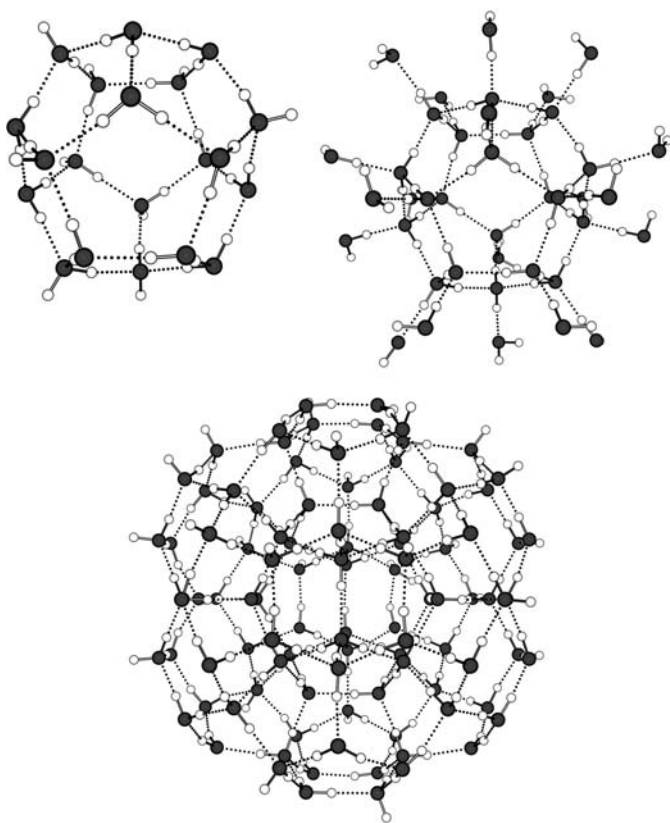


Fig. 9. The free $(\text{H}_2\text{O})_{100}$ water cluster. Top left: the central $(\text{H}_2\text{O})_{20}$ dodecahedron displaying 30 intramolecular hydrogen bonds. Top right: the fully H-bonded vertex-decorated $(\text{H}_2\text{O})_{40}$ dodecahedron (40 hydrogen bonds). Bottom: the full cluster with its 170 intramolecular hydrogen bonds.

Faced with these problems of convergence, a good way to speed up the process is to remove the cluster from its capsule. This considerably reduces the computation time because we are now considering an assembly of only 300 atoms with 200 H-atoms moving onto a 300-D hypersurface. Figure 9 shows the result for this reduced problem that is characterized by: $R_{\text{ext}} = 10.17 \text{ \AA}$, $\rho = 0.678 \text{ g} \cdot \text{cm}^{-3}$ (37.8% compactness), $I_A = 97.1 \times 10^{-42} \text{ kg} \cdot \text{m}^2$, $I_B = 96.2 \times 10^{-42} \text{ kg} \cdot \text{m}^2$, $I_C = 95.7 \times 10^{-42} \text{ kg} \cdot \text{m}^2$ (spherical top), $v_{\text{mol}} = 1666(1) \text{ \AA}^3$, $s_{\text{mol}} = 1918(2) \text{ \AA}^2$, and $\langle EB_{\text{W100F}} \rangle = -21887.3 \text{ kJ} \cdot \text{mol}^{-1}$. If we compare these results with the previous ones, we may notice, as expected, a slight expansion associated to a much lower EB-value. Figure 10 shows as before the histograms for the H-O...O non-bonded angles and the individual O-H...O energies of interaction. We immediately see that we have in hand a pretty good solution as the widest angle is about 14° and the weakest H-bond is about $-13 \text{ kJ} \cdot \text{mol}^{-1}$. The small bump around 8.5° may be indicative that some part of the cluster may be further optimized. Performing the same analysis as before (Fig. 9)

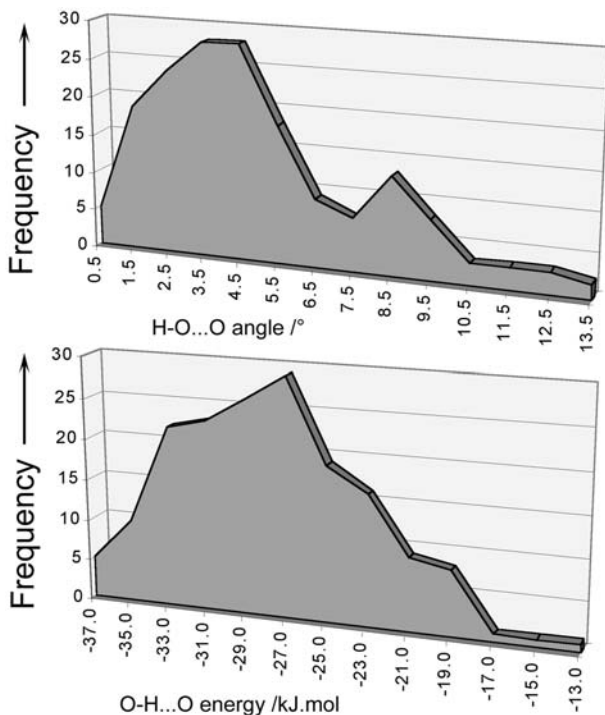


Fig. 10. Angular ($\theta_{\text{H-O}\dots\text{O}}$) distribution function (top) for the H-bond pattern found in the free isolated $(\text{H}_2\text{O})_{100}$ cluster and its associates energetic partition function (bottom).

leads now to a perfectly H-bonded dodecahedron of twenty water molecules. With $\langle EB_{W20F} \rangle = -4124.3 \text{ kJ} \cdot \text{mol}^{-1}$ corresponding to a total of 30 hydrogen bonds, we get $\langle E_{HB} \rangle = (\langle EB_{W20F} \rangle + 20 \times 171.25) / 30 = -23.3 \text{ kJ} \cdot \text{mol}^{-1}$. This is the typical value found in crystalline ice. By adding the twenty other water molecules onto each vertex, we get a $(\text{H}_2\text{O})_{40}$ water cluster characterized by $\langle EB_{W40I} \rangle = -8142.3 \text{ kJ} \cdot \text{mol}^{-1}$ and 50 H-bonds, i.e., $\langle E_{HB} \rangle = (\langle EB_{W40F} \rangle + \langle EB_{W20F} \rangle + 20 \times 171.25) / 20 = -29.7 \text{ kJ} \cdot \text{mol}^{-1}$. At last, after capping by the sixty remaining water molecules we got $\langle E_{HB} \rangle = (\langle EB_{W100F} \rangle + \langle EB_{W40F} \rangle + 60 \times 171.25) / 120 = -28.9 \text{ kJ} \cdot \text{mol}^{-1}$.

CONCLUSION

In summary, we have tried to show that Achim's clusters and nanocapsules are fascinating systems for anyone interested in water structure either as a pure medium ($[(\text{H}_2\text{O})_{100}]$ system) or in contact with cationic species (ammonium and sodium ions). It has to be realized that, for the first times, it is possible to get reliable structural models (onto which we may perform a full statistical analysis) not biased by the use of empirical and/or theoretical potentials. In fact we are at the very beginning of an exciting and rewarding water story, and we may bet that in a very near future, a great amount of new water clusters will be synthesized and analyzed along the lines developed just above. Among systems that are already ready to be studied without any further synthesis or characterization, we may cite the $[\text{H}_2\text{O}]_{40}$ and $[\text{H}_2\text{O}]_{80}$ clusters evidenced in the crystal structures of $[\text{Mo}_{102}\text{O}_{282}(\text{CH}_3\text{COO})_{12}(\text{H}_2\text{O})_{78}] \cdot 110\text{H}_2\text{O}$ [20] and $[\text{Mo}_{132}\text{O}_{372}(\text{H}_2\text{PO}_2)_{30}(\text{H}_2\text{O})_{72}] \cdot 220\text{H}_2\text{O}$ respectively [17]. Concerning the influence of ammonium and/or sodium ions on water structure, we may study the quite new sulfate-based systems such as $(\text{NH}_4)_{72}[\text{Mo}_{132}\text{O}_{372}(\text{SO}_4)_{30}(\text{H}_2\text{O})_{72}] \cdot 200\text{H}_2\text{O}$, $(\text{NH}_4)_{60}[\text{Mo}_{132}\text{O}_{372}(\text{SO}_4)_{18}(\text{CH}_3\text{COO})_{12}(\text{H}_2\text{O})_{72}] \cdot 300\text{H}_2\text{O}$ and $\text{Na}_8(\text{gua})_{52}[\text{Mo}_{132}\text{O}_{372}(\text{SO}_4)_{24}(\text{CH}_3\text{COO})_6(\text{H}_2\text{O})_{72}] \cdot 250\text{H}_2\text{O}$ [27]. Other fascinating systems include the structure of the water hydration shell of Mo_{176} and Mo_{154} wheels or of the Mo_{368} nano-hedgehog. With no doubts, some amazing new results are lurking around these molybdenum-based nanocapsules.

REFERENCES

1. J. Berzelius (1826). *Poggendorfs Ann. Phys. Chem.* **6**, 369.
2. M. T. Pope, *Heteropoly and Isopoly Oxometalates* (Springer-Verlag, Berlin, 1983).
3. M. I. Khan and J. Zubieta (1992). *J. Am. Chem. Soc.* **114**, 10058.
4. A. Müller, E. Krickemeyer, S. Dillinger, H. Bögge, W. Plass, A. Proust, L. Dloczik, C. Menke, J. Meyer, and R. Rohlfing (1994). *Z. Anorg. Allg. Chem.* **620**, 599.

5. A. Müller, W. Plass, E. Krickemeyer, S. Dillinger, H. Bögge, A. Armatage, A. Proust, C. Beugholt, and U. Bergmann (1994). *Angew. Chem. Int. Ed.* **33**, 849.
6. A. Müller, E. Krickemeyer, J. Meyer, H. Bögge, F. Peters, W. Plass, E. Diemann, S. Dillinger, F. Nonnenbruch, M. Randerath, and C. Menke (1995). *Angew. Chem. Int. Ed.* **34**, 2122.
7. A. Müller, E. Krickemeyer, H. Bögge, M. Schmidtman, C. Beugholt, P. Kögerler, and C. Lu (1998). *Angew. Chem. Int. Ed.* **37**, 1220.
8. C.-C. Jiang, Y.-G. Wei, Q. Liu, S.-W. Zhang, M.-C. Shao, and Y.-Q. Tang (1998). *Chem. Commun.*, 1937.
9. A. Müller, M. Koop, H. Bögge, M. Schmidtman, and C. Beugholt (1998). *Chem. Commun.*, 1501.
10. M. Henry (2002). *Chem. Phys. Chem.* **3**, 561.
11. M. Henry (2002). *Chem. Phys. Chem.* **3**, 607.
12. M. Henry (2002). *J. Cluster Sci.* **13**, 437.
13. F. Taulelle and C. Huguenard (2001). *Stud. Surf. Sci. Catal.* **135**, 1414.
14. A. Müller, E. Krickemeyer, H. Bögge, M. Schmidtman, and F. Peters (1998). *Angew. Chem. Int. Ed.* **37**, 3360.
15. M. Henry and A. Müller, *Angew. Chem. Int. Ed.* (submitted).
16. A. Müller, V. P. Fedin, C. Kuhlmann, H. Bögge, and M. Schmidtman (1999). *Chem. Commun.*, 927.
17. A. Müller, S. Polarz, S. K. Das, E. Krickemeyer, H. Bögge, M. Schmidtman, and B. Hauptfleisch (1999). *Angew. Chem. Int. Ed.* **38**, 3241.
18. A. Müller, S. Sarkar, S. Q. N. Shah, H. Bögge, M. Schmidtman, S. Sarkar, P. Kögerler, B. Hauptfleisch, A. X. Trautwein, and V. Schünemann (1999). *Angew. Chem. Int. Ed.* **38**, 3238.
19. A. Müller, E. Beckmann, H. Bögge, M. Schmidtman, and A. Dress (2002). *Angew. Chem. Int. Ed.* **41**, 1162.
20. A. Müller, S. Q. N. Shah, H. Bögge, M. Schmidtman, P. Kögerler, B. Hauptfleisch, S. Leiding, and K. Wittler (2000). *Angew. Chem. Int. Ed.* **39**, 1614.
21. A. Müller, E. Krickemeyer, H. Bögge, M. Schmidtman, S. Roy, and A. Berkle (2002). *Angew. Chem. Int. Ed.* **41**, 3604.
22. A. Müller, H. Bögge, and E. Diemann (2003). *Inorg. Chem. Commun.* **6**, 42.
23. A. Gavezzoti (1983). *J. Am. Chem. Soc.* **105**, 5220.
24. F. Torrens (2001). *Int. J. Mol. Sci.* **2**, 72.
25. I. D. Brown and R. D. Shannon (1973). *Acta Cryst. A* **29**, 266.
26. M. F. Chaplin (1999). *BioPhys. Chem.* **83**, 211.
27. A. Müller, E. Krickemeyer, H. Bögge, M. Schmidtman, B. Botar, and M. O. Talismanova (2003). *Angew. Chem. Int. Ed.* **42**, 2085.